PHYSICAL REVIEW A VOLUME 22, NUMBER 1 JULY 1980

# Improved atomic model for charge transfer in multielectron ion-atom collisions at intermediate energies

C. D. Lin and L. N. Tunnell
*Department of Physics, Kansas State University, Manhattan, Kansas 66506*
(Received 3 December 1979)

Electron capture to the $K$ shell of projectiles from the $K$ and other subshells of multielectron target atoms is studied in the intemediate energy region using the single-active-electron approximation and the two-state, two-center atomic eigenfunction expansion method. It is concluded that the theoretical capture cross section is *not* sensitive to the atomic models used at high collision energies where the projectile velocity $v$ is near or greater than the orbital velocity $v_e$ of the active electron. For $v < v_e$, however, a proper atomic potential such as the Herman-Skillman potential is needed to represent the target atom. The insufficiency of various simple Coulomb model potentials is illustrated. Capture cross sections for a few collision systems are obtained and compared with experimental data when available to illustrate the reliability of the present model.

## I. INTRODUCTION

The electron-transfer process is important in the reaction between charged particles and matter. In the context of fast ion-atom collisions, recent experiments[1-5] have shown that it also plays a very important role in the production of inner-shell vacancies for highly charged incident ions.

In this article we are interested in the theory of single-electron transfer in ion-atom collision in the energy region where the collision velocity $v$ is *not* very small compared with the orbital velocity $v_e$ of the electron to be captured. Theoretical investigations of electron transfer in this intermediate ($v \sim v_e$) energy region for multielectron systems are scarce except for the asymmetric systems. Reading *et al.*[6] and Ford *et al.*[7] have recently extended their early one-center, multistate expansion method, originally developed for Coulomb ionization,[8] to electron-capture problems. The continuous-distorted-wave (CDW) approximation, originally developed for electron transfer at higher collision energies,[9] has recently been applied to electron transfer at lower energies.[10] Both approaches are primarily limited to collisions where capture probabilities are small and thus are not suitable for near-symmetric collisions.

In our recent works[11,12] we have extended the two-center atomic eigenfunction expansion method, originally proposed by Bates,[13] to electron-transfer problems in multielectron ion-atom collisions in the independent electron approximation. In its simplest form, the two-state, two-center atomic expansion method is shown to predict adequately the total $K$-$K$ electron-transfer cross sections for near-symmetric[12] as well as for very asymmetric collisions[11] in certain energy ranges. With a reasonable choice of eikonal phase approximation to describe the scattering between the heavy particles, the method is shown[14] to predict differential capture cross sections in good agreement with experiments. However, these earlier works have certain undesirable limitations which have to be removed before an improved theoretical model for the capture mechanism can be developed. In this article we examine and describe the method of removing these undesirable features of the earlier works.

In generalizing the atomic eigenfunction expansion method to multielectron ion-atom collisions for single-electron-transfer problems, it is desirable in the initial investigation to work in the active-electron approximation by considering the electron that is transferred only; the effects of other passive electrons are initially to be included only in providing appropriate screening. Even within this simple active-electron approximation, there are different degrees of sophistication in approximating the screening function. In our earlier studies[11,12] we investigated the capture of $K$-shell electrons to the $K$ shell of bare projectiles. We represented the potential of the active electron in the initial state by a simple Coulomb potential with a certain effective charge. There are some inherent drawbacks in using such a simple screening function, particularly for near-symmetric collisions. This is to be explained in Sec. III. We will show that the conventional methods of improving the hydrogenic potential by adding a constant outer screening, as often done in the theory of photoionization[15] and in the plane-wave Born approximation (PWBA) theory of Coulomb ionizations,[16] introduces certain inconsistencies. In this paper we will show that a more realistic atomic potential, such as the simple Hartree-Fock-Slater (HFS) potential, is needed in a consistent charge-transfer theory even for the capture of $K$-shell electrons in a near-symmetric collision. This is

 

to be contrasted with the direct Coulomb ionization of $K$-shell electrons in which outer screening is often adequate in describing the effects of outer passive electrons and the HFS potential is considered as an unnecessary luxury.[17] An additional advantage of using a realistic potential is that it allows us to investigate electron capture from other subshells, even from the outermost subshells of most atomic systems. This is possible because the gross features of atomic properties are often adequately described by the HFS model, as has been shown from atomic photoionization studies.[18] Otherwise, we can compare the predictions of this single-electron theory with experimental data to assess the importance of many-electron effects for outershell electrons in a charge-transfer process.

The rest of the structure of this paper is as follows: In Sec. II we briefly describe the basic equations of the two-state, two-center atomic eigenfunction expansion method and give the important equations for later discussions. The difficulties of using simple hydrogenic atomic models are discussed in Sec. III and the method of introducing realistic HFS potentials in a charge-transfer theory is followed. The results of the $K$-$K$ electron-transfer cross sections calculated in different atomic models are compared in Sec. IV A for very asymmetric collisions and in Sec. IV B for near-symmetric collisions. These calculations are also compared with experimental data. In Sec. IV C, we investigate the *target* charge-state dependence of $K$-$K$ electron-transfer cross sections in view that $K$-$K$ charge transfer is often accompanied by simultaneous outer-shell ionizations. This study is important when theoretical calculations are to be compared with experimental data. We also present outer-shell electron-capture cross sections of Ne and Kr by protons and the $L$-shell electron capture of Ar by bare projectiles with nuclear charge from two to five in order to complement the subshell electron-capture cross sections of Ar by protons reported earlier.[19]

## II. SUMMARY OF BASIC EQUATIONS

In this article we are interested in the capture of a *single* electron from a multielectron atom by *structureless* heavy projectiles. The target atom has nuclear charge $Z_A$ and the bare projectile has nuclear charge $Z_B$. (The subscripts $A$ and $B$ are also to be used to denote other quantities referring to the target and to the projectile, respectively.) By adopting an active electron approximation (the validity of this assumption will be further examined in Sec. V), the time dependence of the wave-function $\Psi(\vec{r}, t)$ of the active electron, in a two-state, two-center atomic eigenfunction expansion method is expressed as

$$\Psi(\vec{r}, t) = a(t)\,\phi_A \exp[-i(\tfrac{1}{2}\vec{v}\cdot\vec{r} + \tfrac{1}{8}v^2 t + E_A t)] + b(t)\,\phi_B \exp[-i(-\tfrac{1}{2}\vec{v}\cdot\vec{r} + \tfrac{1}{8}v^2 t + E_B t)] , \quad (1)$$

where $\phi_A$ and $\phi_B$ are initial and final atomic eigenstates, with energies $E_A$ and $E_B$, centered around target $A$ and projectile $B$, respectively. By choosing the origin of the coordinate system at the midpoint of the internuclear axis and adopting a straight line trajectory, substitution of (1) into the time-dependent Schrödinger equation will give a set of coupled first-order differential equations for $[a(t), b(t)]$. For the discussion later, however, it is more convenient to express the coupled equations as

$$i\dot{d}_A = d_B \frac{h_{AB} - S_{AB}h_{BB}}{1-S^2} \exp\left(i\int^t (U_A - U_B)dt\right) , \quad (2a)$$

$$i\dot{d}_B = d_A \frac{h_{BA} - S_{BA}h_{AA}}{1-S^2} \exp\left(-i\int^t (U_A - U_B)dt\right) , \quad (2b)$$

where $d_A(t)[d_B(t)]$ is related to $a(t)[b(t)]$ by a phase transformation. The derivation of (2) and the matrix elements $S_{ij}$ and $h_{ij}$ $(i, j = A, B)$ are given in Ref. 11 and $U_A$ and $U_B$ are

$$U_A = E_A + \frac{h_{AA} - S_{AB}h_{BA}}{1-S^2} , \quad (3a)$$

$$U_B = E_B + \frac{h_{BB} - S_{BA}h_{AB}}{1-S^2} . \quad (3b)$$

They are the "*diabatic* atomic potentials"[20] and are identical to the *diabatic* potential curves in the $v=0$ limit calculated in the two-state linear-combination-of-atomic-orbital (LCAO) approximation.[21] In $U_A$ we note that $E_A$ is the binding energy of the electron in the initial state in the separated-atom limit, and the second term on the right-hand side of (3a) is the additional *distortion* potential induced by the projectile during the collision. Similarly, the second term on the right-hand side of (3b) is the distortion due to the residual target atom when the active electron is attached to the projectile.

The coupled equations (2) form the basis of further discussion. They are to be solved with boundary conditions $d_A(-\infty)=1$, $d_B(-\infty)=0$ for each impact parameter $\rho$ and each collision energy $E$, either by direct numerical integration or by an iterative method. An exact solution of (2) will guarantee the unitarity condition $|d_A(+\infty)|^2 + |d_B(+\infty)|^2 = 1$. The total single-electron-capture cross sections *per atomic subshell* (twofold degeneracy with spin-up and spin-down for a given

spatial quantum number), in atomic units, is obtained from

$$Q = 2\pi \int 2P(1-P)\rho\, d\rho, \tag{4}$$

where $P = P(\rho, E) = |d_B(+\infty)|^2$ is the capture probability calculated in the single-active-electron approximation. The factor $(1-P)$ in the integrand restricts (4) to single-electron transfer only.[22] Equation (4) is valid for capture to a final state which is empty. If the final state is half filled initially (e.g., the $K$ shell of hydrogenlike projectile), then the additional factor 2 in (4) and the factor $(1-P)$ have to be omitted.

## III. ATOMIC POTENTIALS

Within the active-electron approximation, there are still many ways to choose the potentials $V_A$ and $V_B$ in the electronic Hamiltonian $H = -\frac{1}{2}\nabla^2 + V_A(r_A) + V_B(r_B)$, where $r_A(r_B)$ is the distance of the electron from the target (projectile). By limiting ourselves to bare projectiles, we have $V_B = -Z_B/r_B$ exactly in this approximation. On the other hand, the potential $V_A$ for the initial multielectron target atom is often approximated to different degrees of sophistication. In Sec. III A, we comment on the difficulties associated with using the simple hydrogenic potentials for $V_A$ in a charge-transfer theory. To resolve these difficulties requires a more realistic atomic potential which is described in Sec. III B. Numerical results for these various choices of $V_A$ are compared in Sec. IV.

### A. Hydrogenic model potentials

In this subsection we consider the capture of $K$-shell electrons only. Within the hydrogenic approximation, one often chooses $V_A = -Z_A^*/r_A$ where the effective charge $Z_A^* = Z_A - \frac{5}{16}$. This effective charge provides a good description for the potential of the $K$-shell electron near the $K$-shell radius and the corresponding hydrogenic $1s$ wave function is very close to the actual $K$-shell orbital wave function (such as the Hartree-Fock $1s$ wave function). However, the hydrogenic binding energy $-Z_A^{*2}/2$ obtained according to this effective charge deviates substantially from the actual $K$-shell binding energy because the outer screening of the $K$-shell electrons by outer passive electrons is not included. To amend this situation, it is often necessary to replace the hydrogenic binding energy by the experimental $K$-shell binding energy, corresponding to adding a constant potential $V_0$ to the screened hydrogenic potential, $V_A = -Z_A^*/r_A + V_0$. This is the usual approach for accounting the effects of passive electrons for photoionization[15] of $K$-shell electrons, as well as in the PWBA theory of Coulomb ionizations[16] of $K$-shell electrons by charged particles.

In our earlier works on charge-transfer problems, we adopted a similar idea by choosing the experimental $K$-shell binding energy $E_K$ for $E_A$ instead of the hydrogenic value $-Z_A^{*2}/2$ for the asymptotic value of $U_A$ [see Eq. (3a)] in the solution of coupled equations (2), but we purposely neglected the outer screening potential $V_0$ in the definition of $h_{AB}$ and $h_{BB}$ (where the matrix elements involve the operator $V_A$). Thus the outer screening is only partially included in these earlier studies and the time-dependent Schrödinger equation is not solved consistently; the result is that the unitarity condition $|d_A(+\infty)|^2 + |d_B(+\infty)|^2 = 1$ of the two-state approximation is destroyed.

It might seem paradoxical that we purposely included the outer screening partially only to introduce nonunitarity in the calculation. A more careful consideration will show that this is the only way that a constant outer screening can be introduced into the theory. If $V_0$ is included in the evaluation of matrix elements $h_{AB}$ and $h_{BB}$, then it amounts to solving the time-dependent Schrödinger equation with the Hamiltonian

$$H_e = -\tfrac{1}{2}\nabla^2 - \frac{Z_B}{r_B} - \frac{Z_A^*}{r_A} + V_0 \tag{5}$$

exactly in a two-state approximation. Such an exact solution will guarantee unitarity, but the outer screening originally sought to be included is not present at all. This paradox can be understood as follows: By adding $V_0$ to $-Z_A^*/r_A$ in Eq. (5), while providing a proper outer screening for the electron in the initial state, it also introduces an unphysical constant outer screening for the electron in the final state when the electron is attached to the projectile. The result is that the coupling terms, and the "potential" difference $(U_A - U_B)$, are all independent of the $V_0$ added. This of course is to be expected in a consistent theory since the constant $V_0$ added in (5) only redefines the zero energy level of the electronic Hamiltonian and should have no effect on any physical properties.

In our earlier works we recognized that a correct asymptotic value of $(U_A - U_B)$ is important for a charge-transfer theory because this difference appears as an oscillating exponential in the coupled equations; thus we decided to disregard the question of nonunitarity and only included outer screening partially. This is further justified by noting that the unitarity condition is never satisfied in a first-order perturbation theory. However, for near-symmetric collisions, charge-transfer probabilities are not small and the effect of nonunitarity [as measured by the deviation of $|d_A(+\infty)|^2$

$+|d_B(+\infty)|^2$ from unity] might not be negligible, but the effect was never investigated.

To include outer screening properly, a more realistic potential $V_A$ which vanishes asymptotically is required. Before leaving this topic, however, it is interesting to comment on two other simple hydrogenic models where unitarity is preserved, though the models have their other apparent drawbacks: (1) By choosing $V_A=-Z_A^*/r_A$ and $E_A=-\frac{1}{2}Z_A^{*2}$, with $Z_A^*=Z_A-\frac{5}{16}$ consistently in the theory, the unitarity is preserved but $E_A$ deviates significantly from $E_K$. (2) By choosing $V_A=-Z_A^{**}/r_A$ and $E_A=-\frac{1}{2}Z_A^{**2}$, with $Z_A^{**}=(2|E_K|)^{1/2}$, this effective charge gives the correct binding energy $E_K$ but the potential $V_A$ and the initial wave function $\phi_A$ are not accurately represented. In Sec. IV we will compare the calculated cross sections using these two models with the more accurate method described below.

### B. The Herman-Skillman model potentials

The hydrogenic potentials, with or without constant outer screening, do not represent the actual approximate potential of an electron in an atom adequately. A realistic atomic potential should behave like $-Z/r$ for small $r$ and vanish like $-1/r$ (for a neutral atom) as $r$ goes to infinity.

Within the active-electron approximation, a *local* potential in a multielectron atom can be expressed as

$$V(r)=-(Z/r)U(r), \tag{6}$$

where the screening function $U(r)$ has the limiting forms

$$U(r)\to\begin{cases}1, & r\to 0 \quad (7a)\\ I/Z, & r>r_0, \quad (7b)\end{cases}$$

with $(I-1)$ the charge state of the ion and $r_0$ roughly the size of the atom. In this work we choose $V(r)$ to be the Herman-Skillman potential[23] which is similar to the HFS potential except for the cutoff (7b) introduced by Latter.[24] These potentials, together with orbital eigenenergies and orbital wave functions for neutral atoms, have been tabulated numerically.[23] For our purpose it is inconvenient to work with numerical wave functions and potentials in the evaluation of matrix elements $S_{ij}$ and $h_{ij}$; we thus chose to fit the numerical potential for neutral atoms to an analytic form

$$V(r)=-\frac{1}{r}[1+(Z-1)(1+c_1r+c_2r^2+c_3r^3)e^{-\lambda r}]\,. \tag{8}$$

This particular form was chosen for its correct asymptotic behavior and its compatibility to the techniques employed for the evaluation of two-center matrix elements. The radial part of the initial wave function $\phi_A$ is expressed in terms of Slater-type orbitals such that

$$R_{nl}(r)=\sum_i A_i r^{N_i-1}e^{-\rho_i r}, \tag{9}$$

where the parameters $N_i$ and $\rho_i$ were taken from the analytical Hartree-Fock results of Clementi and Roetti.[25] The remaining parameters $A_i$ were left free to absorb any necessary adjustments by diagonizing the radial Hamiltonian. The eigenvalues and orbital wave functions thus obtained are very close to the analytical Hartree-Fock[25] and the numerical Herman-Skillman results.[23] The orbital energies thus calculated, unlike the simple hydrogenic models, are all within 1–2% of the actual experimental energies.

By using the approximate potential (8) for the target atom and its corresponding eigenenergies and eigenfunctions in the two-state approximation, the unitarity condition of the coupled equations is satisfied in an exact numerical calculation. In a two-state approximation for bare-projectile–multielectron-atom collisions, the Herman-Skillman model calculation is theoretically sounder than the different hydrogenic models described in Sec. III A and should be served as the criterion for comparison.

An additional feature of employing realistic model potential is that the method allows us to compute electron capture from subshells other than the $K$ shell. Preliminary results for the capture from every subshell of Ar atoms by protons have been reported elsewhere.[19] We will present some additional results in Sec. IV.

## IV. RESULTS AND DISCUSSIONS

We have applied the two-state atomic eigenfunction expansion model to calculate electron-transfer cross sections for several systems of ion-atom collisions using different atomic models for the target atoms (the projectiles are restricted to bare nuclei) to investigate the dependence of the calculated capture cross sections upon the atomic models used within the active-electron approximation. Comparisons of the calculated $K$-$K$ capture cross sections among different atomic models and with experimental data are presented in Sec. IV A for very asymmetric systems and in Sec. IV B for near-symmetric systems. We also have investigated the dependence of the capture cross sections upon the charge state of the *target* atoms in Sec. IV C. This study is relevant in that $K$-$K$ electron transfer is often accompanied by multiple ionizations of outer electrons in the target atom. Transfer of electrons from the $L$ shell of Ne and

TABLE I. $K$-$K$ electron-capture cross sections (in $10^{-24}$ cm$^2$) per target atom for protons on argon atoms calculated according to different atomic models. Experimental data are obtained from Table I of Macdonald *et al.* (Ref. 26) by dividing by 1.2.

| $E$ (MeV) | $Z^*$ | $Z^{**}$ | Hyd | HS | Expt |
|---|---|---|---|---|---|
| 3 | 3.2 | 17.6 | 11.6 | 7.8 | 22.7 |
| 4 | 6.6 | 25.6 | 14.8 | 11.8 | 21.8 |
| 5 | 9.0 | 27.6 | 17.2 | 14.2 | 16.3 |
| 6 | 10.2 | 25.5 | 17.0 | 15.0 | 14.0 |
| 8 | 9.6 | 18.6 | 12.4 | 12.0 | 8.3 |
| 10 | 7.6 | 12.6 | 7.8 | 7.6 | 4.7 |
| 12 | 5.8 | 8.2 | 5.8 | 5.8 | 2.8 |

the $N$ shell of Kr to protons, and the capture of $L$-shell electrons of Ar atoms by bare projectiles with charge $Z=2$–5 are presented in Sec. IV D. These calculations are compared with experimental data when available.

### A. $K$-$K$ capture cross sections—very asymmetric systems

We first study the $K$-$K$ capture of Ar atoms by protons where the cross sections are very small. In Table I we present the theoretical $K$-$K$ capture cross sections for energetic protons on argon atoms using different atomic models and with experimental results. The experimental values are obtained from the data of Macdonald *et al.*[26] by dividing their tabulated values by 1.2, with the assumption that cross sections for capture to excited states with principal quantum number $n$ follows the $1/n^3$ rule.[27] Among the theoretical calculations, the first two are in the two hydrogenic models described at the end of Sec. IIIA, to be called $Z^*$ and $Z^{**}$ models, respectively. The third one, designated as "Hyd," is the model used in our earlier studies[11,12] where the effective charge $Z^*$ and the binding energy $E_K$ are not chosen consistently. The fourth theoretical calculation, designated as "HS," is obtained by using the Herman-Skillman model potential, as described in Sec. IIIB. Recall that among the theoretical models, only the Hyd model does not satisfy the unitarity condition in an exact numerical calculation, while the HS model is the more realistic one and is to be served as the criterion for comparing the quality of different hydrogenic models.

In comparing the theoretical calculations, we first note that the Hyd and the HS results agree quite well at high energies. This can be understood from the first-order solution of the coupled equations (2).[11] In the limit of small capture probability, we can assume $d_A(t)\equiv 1$; then Eq. (2b) can be integrated directly to obtain electron-capture probability. This first-order perturbation solution (the unitarity condition is not satisfied in this approximation) is governed by the coupling term in Eq. (2b) which is the product of the "dynamic atomic coupling term" $(h_{BA}-S_{BA}h_{AA})/(1-S^2)$ and the "distortion term" $\exp[-i\int^t (U_A-U_B)dt]$. Both terms are oscillatory functions of time $t$. The dynamic atomic coupling term derives its oscillatory character from the $\exp(-\vec{v}\cdot\vec{r})$ factor in the definitions of $h_{BA}$ and $S_{BA}$. This oscillation becomes faster with *increasing* velocity $v$. On the other hand, the distortion term can be written in terms of an integration over $R$ approximately as $\exp(-i/v\int^R [U_A-U_B]dR')$. Its oscillation is more rapid with *decreasing* $v$. Thus we can conclude that a correct kinematic description by including proper electron translational factors is important at higher collision velocities, while a proper account of the dynamics by including suitable distortion is important at slower collision velocities.

In the Hyd and the HS models, the wave functions $\phi_A$ in the two models and hence the dynamic atomic coupling terms are almost identical, resulting in nearly identical capture cross sections at higher energies. At lower energies, the agreement is not as good because the cross section is primarily dominated by the distortion term. While $U_A$ is almost identical for the hydrogenic and the HS models, $U_B$ is noticeably different (see Fig. 1). Referring to Eq. (3b), we notice that the difference in $U_B$ in the two models comes primarily from the difference in $h_{BB}$ (remember $E_B$ is identical in the

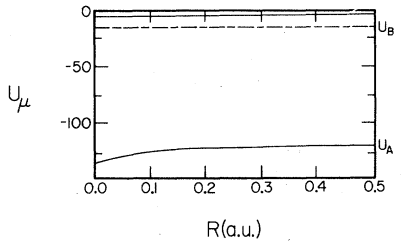


FIG. 1. Diabatic atomic potential curves, as defined in Eqs. (3a) and (3b) for the $H^+$-Ar system using two atomic models for Ar. The lower curve $U_A$ which dissociates to the $K$ shell of Ar at large $R$, does not show any significant dependence on the atomic model potentials chosen. The two upper curves $U_B$, both correspond to H(1$s$) limit at large $R$, show substantial dependence on the atomic model chosen for Ar. The solid line is the result of using Herman-Skillman potential, while the dash-dotted curve represents the result of using screened hydrogenic potential. Only the real part of $U_A$ and $U_B$ are shown. The curves correspond to $V/V_K=\frac{1}{2}$, where $V$ is the projectile velocity and $V_K$ is the Ar $K$-shell velocity. At this energy the imaginary parts of $U_A$ and $U_B$ are small.

two models). This term describes the distortion of the electron in the *projectile* by the different target potential $V_A$ in the HS and Hyd models. Theoretical collision models which do not include the distortion effect would not predict different results for these two atomic models.

The $Z^*$ model also predicts capture cross sections in good agreement with the results of HS model at high energies, but the discrepancy at low energies is much more significant. This is anticipated from the discussion given in the previous paragraph since this model has the correct (in comparison with the HS model) wave function $\phi_A$ but wrong $U_B$. The $Z^{**}$ model does not predict good results in general; its wave function $\phi_A$ is too diffuse and its potential $V_A$ is too weak at small radius; thus its predictions are higher than the HS results over the entire energy region studied.

In comparing the HS results with experimental data in Table I, we notice there is still substantial discrepancy for collision energies away from the velocity matching at 6 MeV, indicating the insufficiency of the present two-state model. At higher energies, the discrepancy probably can be reduced by including target excited and pseudostates in the theoretical model to account for the coupling with direct excitation and ionization channels. These channels would take away the probability amplitude which would otherwise feed back to the charge-transfer channel in the two-state approximation. Study is underway to investigate this speculation. At lower energies, the situation is less clear—the active-electron approximation is usually less applicable at smaller collision energies. Coupling with excitation channels might be important and double-electron processes (like $L$-shell capture accompanied by $K \rightarrow L$ excitations) might not be negligible. These corrections cannot be included without going beyond the single-active-electron approximation. More studies are required to understand the role of each effect.

### B. *K-K* electron-capture cross sections—near-symmetric collisions

We have also investigated the dependence of theoretical $K$-$K$ capture cross sections upon the atomic models used for near-symmetric collisions where the first-order perturbation solution of the coupled equations (2) is no longer valid. In Table II, the $K$-$K$ capture cross sections $\sigma_{KK}$ *per target K-shell electron* for $F^{9+}$+Ar are presented. The entries in this table are mostly for slower collisions where the energies are below the velocity matching $v = v_e$ at $E = 114$ MeV. By comparing the predictions of the three hydrogenic models, it appears that the $Z^*$ model gives best agreement with the HS model. The Hyd model

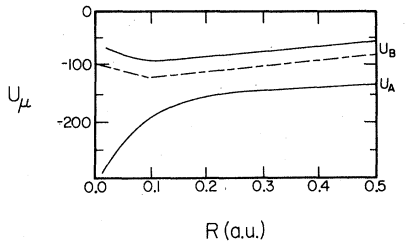


FIG. 2. The same as in Fig. 1, except for $F^{9+}$-Ar system.

used in our previous calculations gave larger $\sigma_{KK}$, especially for lower energies.

This situation can be understood again from the two diabatic potential curves $U_A$ and $U_B$ in these models. In Fig. 2, these curves for the HS and the Hyd model are shown. Similar to Fig. 1, the $U_A$ curve is essentially identical for the two models, but $U_B$ is markedly different. The $U_B$ curve for the Hyd model is lower because of the stronger distortion (measured primarily by $h_{BB}$) of the final state by the unreasonable large hydrogenic potential $-Z_A^*/r_A$. Because of its larger separation $(U_B - U_A)$, the $\sigma_{KK}$ predicted by the HS model is smaller than that predicted by the Hyd model at the same energy. In the $Z^*$ model, the $U_B$ curve is essentially identical to the $U_B$ curve for the Hyd model because of identical $E_B$ and $h_{BB}$ [see Eq. (3a)] used, but its $U_A$ curve is uniformly *lower* by an amount $(Z_A^{*2}/2 - |E_K|)$, corresponding to the difference used in the asymptotic values for $E_A$ in the two models. The net effect is that the separation between $U_A$ and $U_B$ curves in the $Z^*$ model is closer to the corresponding separation in the HS model, and thus the calculated $\sigma_{KK}$ in the $Z^*$ model is in better agreement with the $\sigma_{KK}$ obtained in the HS model.

In Table II, we did not present the "experimental" $\sigma_{KK}$ for comparison. Since these experimental $\sigma_{KK}$ have to be *deduced* from the charge-state

TABLE II. $K$-$K$ electron-capture cross sections (in $10^{-20}$ cm$^2$) per target $K$ electron for $F^{9+}$ on Ar atoms calculated according to different atomic models.

| $E$ (MeV) | $v/v_K$ | $Z^*$ | $Z^{**}$ | Hyd | HS |
|---|---|---|---|---|---|
| 20 | 0.42 | 4.2 | 21.3 | 23.1 | 5.6 |
| 30 | 0.51 | 7.6 | 42.4 | 34.7 | 10.0 |
| 36 | 0.56 | 11.2 | 52.0 | 38.6 | 16.0 |
| 46 | 0.64 | 17.1 | 55.0 | 40.4 | 22.0 |
| 56 | 0.70 | 21.2 | 59.3 | 38.7 | 26.0 |
| 66 | 0.76 | 23.2 | 55.3 | 35.0 | 27.0 |
| 80 | 0.84 | 23.5 | 47.5 | 30.0 | 27.0 |
| 114 | 1.00 | 19.1 | 30.1 | 20.0 | 21.0 |
| 256.5 | 1.50 | 4.9 | 5.1 | 4.1 | 4.7 |
| 456 | 2.00 | 0.98 | 0.84 | 0.68 | 0.77 |

dependence of the gas target x-ray measurements, additional assumptions on the fluorescence yields and the contributions from other processes like direct excitation, ionization, and charge transfer to excited states are needed. These matters will be examined in a separate paper[28] and comparison between HS results and deduced experimental $\sigma_{KK}$ for gas targets will be presented there.

When solid targets are used, the fluorescence yields have been found to be nearly independent of the charge state of the projectiles.[29] For near-symmetric collisions, $\sigma_{KK}$ dominates over all other $K$-vacancy creation processes; thus the assumption of constant cross sections (independent of the charge state of the projectiles) due to these other processes will not affect significantly the deduced $\sigma_{KK}$. In Fig. 3 we show the experimental $K$-$K$ electron-transfer cross sections per target *atom* for $F^{9+}$+Si from Tawara *et al.*[30] and the two theoretical calculations, the dashed line from the Hyd model and the solid line from the HS model. Although the two theoretical models agree with each other and with experimental data at higher collision energies, the Hyd model does show significant discrepancy with experimental data at lower energies. On the other hand, the HS model agrees with experimental data quite well even at lower energies. The large discrepancy in the two theoretical results indicates the importance of the distortion term in a charge-transfer theory at lower energies. It also indicates that the simple-minded hydrogenic model is very inadequate for

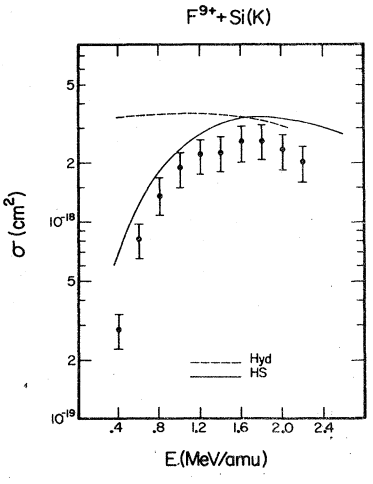


FIG. 3. $K$-$K$ electron-transfer cross sections in $F^{9+}$ on Si collisions. Experimental data are due to Tawara *et al.* (Ref. 30). Two theoretical curves are shown—the dashed curve corresponds to the earlier calculations (Ref. 21) using screened hydrogenic potential for Si atom; the solid curve is the result of using Herman-Skillman potential for Si.

$v < v_e$. To see the reason for this discrepancy, we compare in Fig. 4 the $U_A$ and $U_B$ curves for these two models. Note that the $U_B$ curves in the models converge to the same limit only at very large $R$, and the discrepancy in the smaller $R$ region accounts for the difference in the calculated $K$-$K$ electron-transfer cross sections at lower energies shown in Fig. 3.

### C. Target charge-state dependence of $K$-$K$ electron-transfer cross sections

In a violent ion-atom collision, inner-shell vacancies are often created with simultaneous multiple outer-shell ionizations, as shown by the rich structure of the resulting x-ray lines on the high-energy side of the characteristic x ray.[31] These satellites, in a typical experiment, are often integrated to give the total measured x-ray production cross sections for a given incident projectile. Comparison of our present single-electron model calculations with these integrated measurements is meaningful only if the $K$-vacancy production cross sections are independent of the degree of outer-shell ionization of the target atoms. In a realistic many-electron theory, cross sections for simultaneous $K$-$K$ electron transfer and multiple outer-shell ionization for each possible final-state configuration have to be computed, the results are then added up in order to compare with the integrated experimental data. Such a theory is obviously beyond our reach at the present stage. Our model essentially assumes that outer-shell ionization occurs before the $K$-$K$ electron transfer event and $\sigma_{KK}$ is essentially independent of how many outer electrons are ionized.

To check the validity of this assumption, we calculate $\sigma_{KK}$ for $F^{9+}$+$Ar^{q+}$ for $q=0$, 7, 10, and 13 using the HS model. The results are present in Table III for four collision energies. Notice that there is no significant change in the calculated

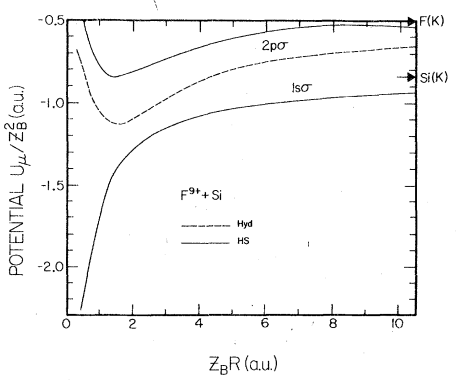


FIG. 4. Diabatic atomic potential curves relevant to the $K$-$K$ charge transfer $F^{9+}$+Si collisions (see Fig. 1 for figure caption).

TABLE III. Target charge-state dependence of $K$-$K$ capture cross sections for $F^{9+} + Ar^{q+*}$. The cross sections are shown in units of $10^{-20}$ cm$^2$ per target $K$ electron.

| | | Target charge state $q$ | | | |
|---|---|---|---|---|---|
| $E$ (MeV) | $v/v_K$ | $0^+$ | $7^+$ | $10^+$ | $13^+$ |
| 20 | 0.42 | 5.2 | 5.8 | 5.6 | 5.3 |
| 36 | 0.57 | 14.5 | 16.1 | 15.5 | 13.6 |
| 66 | 0.77 | 24.9 | 25.8 | 25.5 | 24.3 |
| 114 | 1.01 | 18.8 | 19.0 | 18.9 | 18.7 |

$\sigma_{KK}$ upon the charge state $q$ of Ar investigated. In a typical $F^{9+}$+Ar collision in the energy range shown in Table III, the average charge state of Ar after the collision is found to be about nine.[4] Since the Ar 1$s$ wave function is hardly modified by the outer-shell ionization, if $(U_A - U_B)$ is nearly independent of $q$, then $\sigma_{KK}$ calculated would be also nearly independent of $q$. To illustrate this point, the $U_A$ and $U_B$ curves for $F^{9+}$+$Ar^{q+}$ are presented in Fig. 5 for $q = 0$, 7, and 13. It is noted that although both $U_A$ and $U_B$ shift downward for increasing $q$, the difference $(U_A - U_B)$ remains nearly independent of $q$; the calculated $\sigma_{KK}$ thus remain nearly constant.

### D. Electron capture from subshells other than the $K$ shell

The Herman-Skillman model provides a satisfactory description of the potential throughout the atom in a multielectron atom, thus the present model can be used to study the transfer of electrons from various subshells of the atom if the Herman-Skillman potential is used for the target potential $V_A$. In this section we study the transfer of electrons from the outermost subshells of neon and krypton atoms by protons; the results are compared with experimental *total* charge-transfer cross sections. It is expected that the present two-state approximation is adequate because the transfer is dominated by the capture to the ground state of the projectile from the outermost subshells of the target, capture to the excited states of the projectile, or from the inner shells of the target is not expected to make substantial contribution in this energy region.

In calculating capture from $np$ subshells, the rotation of the internuclear axis is included in the fashion of McElroy.[32] The results of our calculations are shown in Fig. 6 for proton energies ranging from 2–200 keV. Total experimental charge-transfer cross sections, shown in solid lines, are obtained from the compilation of Tawara and Russek.[33] Theoretical results for the capture from each subshell are shown in dashed lines, while the total capture cross sections from the $N$ shell of Kr and the $L$ shell of Ne are shown in dash-dot lines. There is no experimental subshell capture

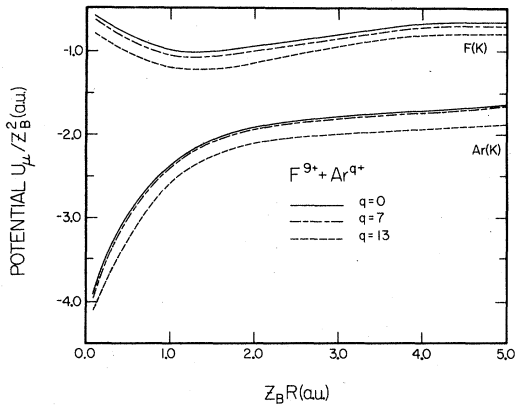


FIG. 5. Diabatic atomic potential curves for $F^{9+}$-$Ar^{9+}$ system for $q = 0$, 7, 13. Both the upper and lower curves for a given $q$ become more negative with increasing $q$, but the difference in the two curves does not change significantly with $q$.

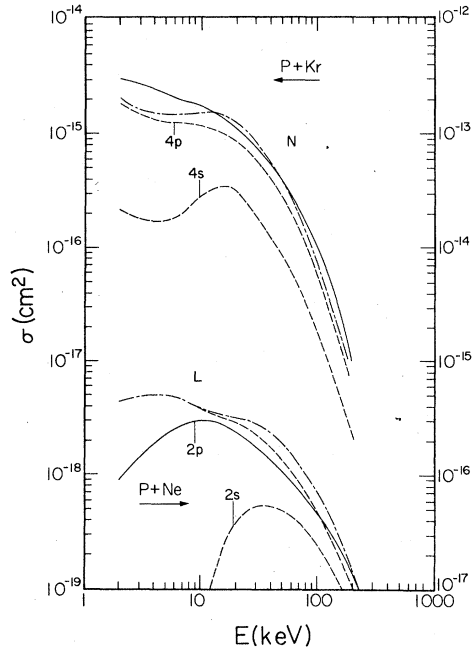


FIG. 6. Electron-capture cross sections from the outer shells of neons and of kryptons by protons. Experimental total capture cross sections, shown in solid lines, are obtained from the compilation of Ref. 33. Total calculated theoretical cross sections from the $L$ shell of neon and from the $N$ shell of kryptons are shown in dash-dot lines, while the contribution from individual subshells is shown in dashed lines.

cross section to compare with the present calculations. By comparing the total electron-transfer cross sections, we notice that the present calculations agree quite well with experimental data except for the $p$+Ne data below 10 keV, where the experimental data show faster drop than the theoretical calculations with decreasing energies. Notice that for $p$+Ne this energy region is probably below where the present model is applicable. The $2p$ binding energy for Ne is 21.6 eV, while the $4p$ binding energy for Kr is 14.0 eV. Since the present atomic model is expected to be valid near the velocity matching region or where the cross sections peak, the region of validity extends to lower proton energies for $p$+Kr collisions than for $p$+Ne collisions. In the lower velocity region where the present model fails, the adiabatic molecular effect and many-electron effects such as exchange symmetry and electron correlation are probably both important.

We have also investigated the capture of $L$-shell electrons of Ar atoms by bare projectiles with nuclear charge $Z_B = 1$–5. This type of projectile charge-dependence study has been done for the capture from the $K$ shell of one-electron[34] and multielectron atoms,[35] but not for the capture from other subshells. In Fig. 7 we show the results of these calculations. The calculated $L \to K$ electron-transfer cross sections are shown for three collision energies—at 200, 400, and 600 keV/amu. Dots represent the calculated values while the lines are drawn to guide the eyes. Notice that the cross sections peak and flatten out near $Z_B = 5$, where the binding energy of hydrogenlike boron is near degenerate with the $L$-shell binding energy of Ar. For higher $Z_B$, capture from the $L$ shell of Ar to the $L$ shell of the projectiles will become important and the $L$-$K$ capture cross sections will drop with increasing $Z_B$. Experimental study of the $L$-shell capture is scarce. The only experiment we know is the $L$-shell capture of Ar by protons by Rødbro *et al.*[35] Our calculations agree reasonably well with their results, as shown in a previous communication.[19]

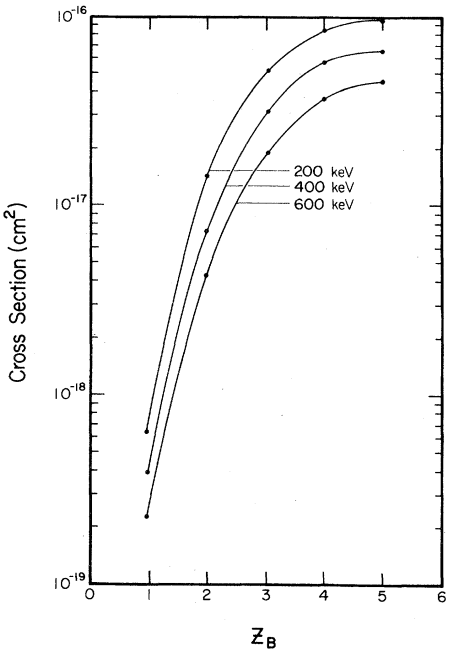


FIG. 7. Capture cross sections of Ar $L$-shell electrons by bare projectiles with $Z_B = 1$–5 at three different energies: 200, 400, and 600 keV/amu.

## V. DISCUSSIONS

A valid charge-transfer theory for multielectron ion-atom collisions requires a proper treatment of the collision dynamics and electron-electron interactions of all the electrons in the system. Under the fast-collision conditions, we neglect the relaxation of passive electrons during the collision and consider only the single active electron which is transferred. Within the two-state, two-center atomic eigenfunction expansion method, we investigated the dependence of the calculated electron-capture cross sections upon the target atomic models used for the active electron. Our results indicate that the calculations are not very sensitive to the atomic models used for high collision energies in which $v \geq v_e$, whether the collision system is very asymmetric or near symmetric. The small discrepancy between experimental $K$-shell capture cross sections and the present theoretical calculations is most likely due to the insufficiency of the two-state collision model rather than the single active-electron approximation. At $v \gg v_e$, charge-transfer cross section is very small and coupling with excitation and ionization channels are probably important.

At lower collision energies the situation is less clear. For near-symmetric collisions, our results in Fig. 3 for $F^{9+}$+Si($K$) shows that good agreement between theoretical and experimental $\sigma_{KK}$ can still be obtained by the present two-state and the active-electron approximation, even down to $v/v_K = 0.4$ (at 400 keV/amu for $F^{9+}$). In this case, the two-state approximation is likely to hold since the effect of other channels which have small cross sections is not expected to change the big $\sigma_{KK}$ channel substantially. Thus the agreement between theory and experiment indicates that the active-electron approximation is probably still valid. For less symmetric systems like $F^{9+}$ +Ar($K$), as will be shown elsewhere,[28] the agree-

ment of $\sigma_{KK}$ between theory and "experiment" is less satisfactory. We tend to believe that the discrepancy comes primarily from the way experimental $\sigma_{KK}$ has been deduced. A separate article will be addressed to this problem. For the very asymmetric collisions like $p+\mathrm{Ar}(K)$, the discrepancy between theoretical two-state calculations and experimental data is more difficult to unravel. In the $v<v_K$ region, direct $K$-shell ionization and capture from $L$ shell are all three orders of magnitude larger than $\sigma_{KK}$. It is likely that two-step processes can modify the present simple two-state results. A theoretical model based upon many-electron wave functions which includes intershell effects is needed to explore the origin of the discrepancy.

In summary, we study the dependence of theoretical electron-transfer cross sections upon the atomic models used in describing a multielectron atom. We conclude that a realistic Herman-Skillman atomic model is needed for collisions in which $v \leq v_e$. For higher collision energies, the results are not very sensitive to atomic models.

ACKNOWLEDGMENT

This work is supported in part by the Division of Chemical Sciences, U. S. Department of Energy. C.D.L. is also partially supported by Alfred P. Sloan Foundation. Part of the numerical calculations in this work were performed at Argonne National Laboratory through Argonne University Association. The authors wish to thank Dr. K. T. Lu and Dr. K. T. Cheng for their assistance.

[1]R. K. Gardner, T. Gray, P. Richard, C. Schmiedekamp, K. A. Jamison, and J. M. Hall, Phys. Rev. A 19, 1896 (1979).
[2]J. R. Macdonald, L. M. Winters, M. D. Brown, L. D. Ellsworth, T. Chiao, and E. Pettus, Phys. Rev. Lett. 30, 251 (1973).
[3]C. W. Woods, R. L. Kauffman, K. A. Jamison, N. Stolterfoht, and P. Richard, Phys. Rev. A 13, 1358 (1976).
[4]F. Hopkins, R. Brenn, A. Whittemore, N. Cue, V. Dutkiewicz, and R. P. Chaturvedi, Phys. Rev. A 13, 74 (1976).
[5]F. D. McDaniel, J. L. Duggan, G. Basbas, P. D. Miller, and G. Lapicki, Phys. Rev. A 16, 1375 (1977).
[6]J. F. Reading, A. L. Ford, G. L. Swafford, and A. Fitchard, Phys. Rev. A 20, 130 (1979).
[7]A. L. Ford, J. F. Reading, and R. L. Becker, J. Phys. B 12, 491 (1979).
[8]G. L. Swafford, J. F. Reading, A. L. Ford, and E. Fitchard, Phys. Rev. A 16, 1329 (1977) and references therein.
[9]I. M. Cheshire, Proc. Phys. Soc., London 84, 89 (1964).
[10]D. Belkic, R. Gayet, and A. Salin, Phys. Rep. 56, 280 (1979).
[11]C. D. Lin, S. C. Soong, and L. N. Tunnell, Phys. Rev. A 17, 1646 (1978).
[12]C. D. Lin, J. Phys. B 11, L185 (1978).
[13]D. R. Bates, Proc. R. Soc. London, Ser. A 274, 294 (1958).
[14]C. D. Lin and S. C. Soong, Phys. Rev. A 18, 499 (1978).
[15]H. A. Bethe and E. E. Salpeter, *Quantum Mechanics of One- and Two-Electron Atoms* (Springer, Berlin, 1957).
[16]See D. Madison and E. Merzbacher, in *Atomic Inner-Shell Processes*, edited by B. Crassemann (Academic, New York, 1975), Vol. I.
[17]D. H. Madison and S. T. Manson, Phys. Rev. A 20, 825 (1979); O. Aashamar and L. Kochbach, J. Phys. B 10, 869 (1977).
[18]U. Fano and J. W. Cooper, Rev. Mod. Phys. 40, 441 (1968).
[19]C. D. Lin and L. N. Tunnell, J. Phys. B 12, L485 (1979).
[20]J. B. Delos and W. R. Thorson, J. Chem. Phys. 70, 1774 (1979). Our diabatic states here correspond to their class-$F$ states.
[21]C. D. Lin, J. Phys. B 11, L595 (1978).
[22]The factor $(1-P)$ in (4) was not implemented in our previous calculations. Within the present model it is important to include this factor to ensure that only single-electron transfer is calculated.
[23]F. Herman and S. Skillman, *Atomic Structure Calculations* (Prentice-Hall, Englewood Cliffs, N. J., 1963).
[24]R. Latter, Phys. Rev. 99, 510 (1955).
[25]E. Clementi and C. Roetti, At. Data Nucl. Data Tables 14, 177 (1974).
[26]J. R. Macdonald, C. L. Cocke, and W. W. Eidson, Phys. Rev. Lett. 32, 648 (1974).
[27]M. R. C. McDowell and J. P. Coleman, *Introduction to the Theory of Ion-Atom Collisions* (North-Holland, Amsterdam, 1970), p. 379; see alto T. G. Winter and C. C. Lin, Phys. Rev. A 10, 2141 (1974).
[28]J. R. Macdonald and C. D. Lin (unpublished).
[29]H. Tawara, P. Richard, T. Gray, P. Pepmiller, J. R. Macdonald, and R. Dillingham, Phys. Rev. A 19, 2131 (1979).
[30]H. Tawara, P. Richard, T. Gray, J. Newcomb, K. A. Jamison, C. Schmiedekamp, and J. M. Hall, Phys. Rev. A 18, 1373 (1978).
[31]For example, see Sec. 2.3.3 of P. Richard, in *Atomic Inner-Shell Processes*, edited by B. Crassemann (Academic, New York, 1975), Vol. I; see also C. L. Cocke, Phys. Rev. A 20, 749 (1979).
[32]M. B. McElroy, Proc. Roy. Soc. London Ser. A 272, 542 (1963).
[33]H. Tawara and A. Russek, Rev. Mod. Phys. 45, 178 (1973).
[34]See, e.g., H. Ryufuku and T. Watanabe, Phys. Rev. A 19, 1538 (1979) and references therein.
[35]M. Rødbro, E. H. Pedersen, C. L. Cocke, and J. R. Macdonald, Phys. Rev. A 19, 1936 (1979).